Journal of Glaciology

Cambridge University Press

THIS MANUSCRIPT HAS BEEN SUBMITTED TO THE JOURNAL OF GLACIOLOGY AND HAS NOT BEEN PEER-REVIEWED.

The effect of uncertainties in creep activation energies on modeling ice flow and deformation

Journal:	*Journal of Glaciology*
Manuscript ID	Draft
Manuscript Type:	Article
Date Submitted by the Author:	n/a
Complete List of Authors:	Ranganathan, Meghana; Georgia Institute of Technology, School of Earth and Atmospheric Sciences; MIT, Department of Earth, Atmospheric and Planetary Sciences Minchew, Brent; Massachusetts Institute of Technology, Department of Earth, Atmospheric and Planetary Sciences
Keywords:	Ice rheology, Ice-sheet modelling, Antarctic glaciology, Glacier flow, Glacier modelling
Abstract:	Ice deformation is commonly represented by a power-law constitutive relation, Glen's Flow Law, where deformation (strain) rate equals stress raised to the power n and multiplied by a flow-rate parameter A. Glen's Law represents bulk ice rheology as a single power-law even though multiple mechanisms, each with their own power-law relation and parametric values, act together during viscous deformation (creep) of ice. The relative importance of different creep mechanisms in naturally-deforming ice sheets controls the parameters n and A in Glen's Flow Law. We couple a composite flow law that explicitly represents individual

	deformation mechanisms with models for ice temperature and grain size to estimate the dominant deformation mechanism in the Antarctic Ice Sheet. We demonstrate that uncertainties in creep activation energies produce significant uncertainties in the dominant deformation mechanism, and thus values of A and n. Minor variations in the activation energy values (<10% or <5 kJ/mol) can change the dominant creep mechanism, causing n to vary between 1.8<n<4. We propose a way of using observational inferences of the stress exponent n to recalibrate activation energy values in ice sheet models. This enables an improved understanding of the fundamental mechanisms of ice deformation and the controls on ice flow.

The effect of uncertainties in creep activation energies on modeling ice flow and deformation

Meghana Ranganathan[1,2], Brent Minchew[1]

[1]*Department of Earth, Atmospheric and Planetary Sciences, Massachusetts Institute of Technology, Cambridge, MA, USA*

[2]*School of Earth and Atmospheric Sciences, Georgia Institute of Technology, Atlanta, GA, USA*

Correspondence: Meghana Ranganathan <meghanar@ucar.edu>

ABSTRACT. Ice deformation is commonly represented by a power-law constitutive relation, Glen's Flow Law, where deformation (strain) rate equals stress raised to the power n and multiplied by a flow-rate parameter A. Glen's Law represents bulk ice rheology as a single power-law even though multiple mechanisms, each with their own power-law relation and parametric values, act together during viscous deformation (creep) of ice. Therefore, the relative importance of different creep mechanisms in naturally-deforming ice sheets controls the parameters n and A in Glen's Flow Law. Here, we couple a composite flow law that explicitly represents individual deformation mechanisms with models for ice temperature and steady-state grain size to estimate the dominant deformation mechanism in the Antarctic Ice Sheet. We demonstrate that uncertainties in activation energies for creep produce significant uncertainties in the dominant deformation mechanism, and thus values of A and n. Minor variations in the values of activation energy (< 10 % or < 5 kJ mol^{-1}) can change the dominant creep mechanism, causing n to vary between $1.8 \leqslant n \leqslant 4$. We propose a way of using observational inferences of the stress exponent n to recalibrate values of activation energy in ice sheet models. This enables an improved understanding of the fundamental mechanisms of ice deformation and the controls on ice flow.

INTRODUCTION

Mass loss from ice sheets is partially controlled by the rate of grounded ice flow to the ocean (Rignot and others, 2002; Scambos, 2004; Wingham and others, 2009; Gudmundsson and others, 2019; King and others, 2020; De Rydt and others, 2021). The rate of ice flow is strongly dependent upon ice viscosity, which depends on multiple creep mechanisms of ice deformation. For each of these mechanisms, the relationship between applied stress and the rate of ice deformation can be parameterized through a power-law constitutive relation, similar in form to Glen's Flow Law (Glen, 1955), and given in scalar form as:

$$\dot{\epsilon}_{e_i} = A_i \tau_e^{n_i} \tag{1}$$

where i denotes the index for the ith mechanism of deformation, $\dot{\epsilon}_{e_i}$ is the effective strain rate attributable to that mechanism, A_i is the flow-rate parameter, τ_e is the applied effective deviatoric stress, and n_i is the viscous stress exponent. The effective strain rate is defined as the square root of the second invariant of the strain rate tensor ϵ_{jk} and the effective stress τ_e is the square root of the second invariant for the deviatoric stress tensor τ_{jk}. The prefactor A_i scales according to a variety of factors described later and the strength of crystallographic preferred orientation, or fabric, which drives anisotropy in the ice.

While all deformation mechanisms are active at all times, the relative contribution of each mechanism to the bulk (total) deformation varies based on conditions in the ice, such as ice temperature, grain size, and stress (Duval and others, 1983; Pimienta and Duval, 1987; Goldsby and Kohlstedt, 1997b; Montagnat and Duval, 2000; Goldsby and Kohlstedt, 2001; Fan and others, 2020). One way of modeling the effect of multiple deformation mechanisms on bulk ice deformation is to construct a composite flow law wherein the total rate of deformation is the sum of the strain rates contributed by each deformation mechanism (Lliboutry, 1969; Smith and Morland, 1981; Goldsby and Kohlstedt, 2001; Pettit and Waddington, 2003). Goldsby and Kohlstedt (2001) proposes the following composite flow law from results of laboratory experiments:

$$\dot{\epsilon} = \dot{\epsilon}_{\text{diff}} + \left[\frac{1}{\dot{\epsilon}_{\text{basal}}} + \frac{1}{\dot{\epsilon}_{\text{gbs}}} \right]^{-1} + \dot{\epsilon}_{\text{dis}} \tag{2}$$

representing the following deformation mechanisms: diffusion creep ($\dot{\epsilon}_{\text{diff}}$) describes flow by the diffusion of point defects in the crystalline lattice, grain-boundary sliding ($\dot{\epsilon}_{\text{gbs}}$) describes flow in which the movement occurs in the grain boundaries, dislocation creep ($\dot{\epsilon}_{\text{dis}}$) describes flow by the movement of line defects within the lattice, and basal sliding ($\dot{\epsilon}_{\text{basal}}$) describes slip along basal planes that accommodates grain-boundary sliding.

Of the four mechanisms represented in Eq. 2, diffusion creep and basal slip should be negligible in existing glaciers and ice sheets. Diffusion creep is negligible by comparison to other creep mechanisms at stresses and ice grain sizes found in natural ice sheets and glaciers (Duval and others, 1983; Goldsby and Kohlstedt, 1997b,a). Similarly, Goldsby and Kohlstedt (2001) finds that basal slip is rate-controlling only at stresses lower than are found in the dynamic regions of glaciers, making grain-boundary sliding the dominant component of the bracketed term in Eq. 2. We can therefore simplify Eq. 2 to represent the mechanisms likely active in the deforming regions of fast-flowing (> 30 m/yr) glacier ice:

$$\begin{aligned}\dot{\epsilon} &= \dot{\epsilon}_{\text{dis}} + \dot{\epsilon}_{\text{gbs}} && \text{(3a)}\\ &= A^{\pm}_{\text{dis}}\tau_e^{n_{\text{dis}}} + A^{\pm}_{\text{gbs}}\tau_e^{n_{\text{gbs}}} && \text{(3b)}\end{aligned}$$

in which $A^{\pm}_{\text{dis}}$ is the flow-rate parameter for dislocation creep, $A^{\pm}_{\text{gbs}}$ is the flow-rate parameter for grain-boundary sliding, and the superscript $\pm$ indicates values for warm $+$ and cold $-$ ice, as defined later. Similarly for n_{dis} and n_{gbs} but, consistent with laboratory experiments, without reference to temperature. The stress exponents are estimated to be $n_{dis} = 4$ and $n_{gbs} = 1.8$ (Goldsby and Kohlstedt, 2001). The flow-rate parameters are expanded as Arrhenius relations

$$\begin{aligned}A^{\pm}_{\text{dis}} &= A^{\pm}_{0_{\text{dis}}} \exp\left\{\frac{-Q^{\pm}_{\text{dis}}}{RT}\right\} && \text{(4a)}\\ A^{\pm}_{\text{gbs}} &= A^{\pm}_{0_{\text{gbs}}} d^{-m} \exp\left\{\frac{-Q^{\pm}_{\text{gbs}}}{RT}\right\} && \text{(4b)}\end{aligned}$$

where $A^{\pm}_{0_i}$ is the flow-rate parameter prefactor, $Q^{\pm}_i$ is the activation energy, R is the ideal gas constant, T is (absolute) ice temperature, d is ice grain size, and $m = 1.4$ is the grain size exponent found by Goldsby and Kohlstedt (2001). The parameters $A^{\pm}_0$ and $Q^{\pm}$ for dislocation creep and grain-boundary sliding each have two values, one for high (superscript $+$) temperatures (262 K $< T \leqslant 273$ K) and one for low (superscript $-$) temperatures ($T \leqslant 262$ K), as a way of parameterizing an observed acceleration in strain-rate at high temperatures (Barnes and others, 1971; Cuffey and Paterson, 2010). These parameters were experimentally determined in Goldsby and Kohlstedt (2001) and have been modified by Kuiper and others (2020b) (Table 1). Hereafter, we drop the superscripts $+$, $-$, and $\pm$ except where necessary in the interest of clarity.

Table 1. Rheological parameters for dislocation creep and grain-boundary sliding presented by Kuiper and others (2020a), who adapted them from Goldsby and Kohlstedt (2001).

Parameter	Value	Unit
$A^{+}_{0_{\mathrm{dis}}}$	6.96×10^{23}	MPa$^{-\mathrm{n_{dis}}}$ s^{-1}
$A^{-}_{0_{\mathrm{dis}}}$	5×10^{5}	MPa$^{-\mathrm{n_{dis}}}$ s^{-1}
Q^{+}_{dis}	155×10^{3}	J mol^{-1}
Q^{-}_{dis}	64×10^{3}	J mol^{-1}
$A^{+}_{0_{\mathrm{gbs}}}$	8.5×10^{37}	MPa$^{-\mathrm{n_{gbs}}}$ m^{m} s^{-1}
$A^{-}_{0_{\mathrm{gbs}}}$	1.1×10^{2}	MPa$^{-\mathrm{n_{gbs}}}$ m^{m} s^{-1}
Q^{+}_{gbs}	250×10^{3}	J mol^{-1}
Q^{-}_{gbs}	70×10^{3}	J mol^{-1}

In these representations of the flow-rate parameters, the values are dependent only on temperature (and the associated kinetic parameters). Anisotropy can be explicitly represented by allowing A_i to be a second-order tensor. Because we consider only scalar A_i in Eq. 1, we do not explicitly account for anisotropy but do account for its influence on the balance of creep mechanisms later in this study by considering a distribution of values of A_i that encompass all known values for an enhancement factor that multiplies A_i (Hudleston, 2015; Minchew and others, 2018).

There remains significant uncertainty in the parameters underlying A_{dis} and A_{gbs}, in particular the activation energies for creep and the prefactors, due to the difficulty in experimentally determining the kinetics of ice deformation and the fact that these parameters have only been determined in a handful of laboratory experiments at specific ice conditions (for example, small grain sizes and fixed ice temperatures). Therefore, it is not presently clear how broadly applicable these laboratory values are to naturally deforming ice. Zeitz and others (2021) compiled studies estimating the activation energy for creep and found values ranging from $Q = 43 - 193$ kJ mol^{-1} (e.g. Weertman (1955); Glen (1955); Jellinek and Brill (1956); Raraty and Tabor (1958); Mellor and Smith (1967); Mellor and Testa (1969b,a); Muguruma (1969); Barnes and others (1971); Goldsby and Kohlstedt (1997b); Treverrow and others (2012); Qi and others (2017); Saruya and others (2019)), a significant range in the value of an exponent. The prefactors are generally calibrated based on the activation energies and the value of the stress exponent n, which is also uncertain, with a canonical range of $1.8 \leqslant n \leqslant 4$ (Jezek and others, 1985; Budd and Jacka, 1989; Cuffey and Paterson, 2010; Bons and others, 2018; Millstein and others, 2022).

Uncertainties in the flow-rate parameter values create significant uncertainties in flow projections due to its multiplicative effect on the rate of deformation (Zeitz and others, 2020). These uncertainties also have major implications for how we model ice flow in large-scale numerical simulations. Presently, ice flow is virtually always modeled with a single-power law constitutive relation, Glen's Flow Law, where $\epsilon_e = A\tau^n$, with $n = 3$ commonly assumed and A calibrated from a combination of field and laboratory studies. Physically, the values of A and n in Glen's Flow Law represent some combination of dislocation creep and grain-boundary sliding (Eq. 3). Therefore, the values of A_{dis} and A_{gbs} not only dictate the enhancement to the overall deformation rate from ice, such as ice temperature and grain size and orientation (fabic), they also provide constraints on the appropriate parameters to apply to Glen's Flow Law in ice-flow models. This point is illustrated by the composite flow law (Equation 3b), where it can be seen that the values of the flow-rate parameters partially control the magnitude of contributions from either deformation mechanism, and thus their relative contributions to ice viscosity. For example, decreasing the ratio of A_{dis} and A_{gbs} will generally lead to grain-boundary sliding having a larger contribution to overall ice deformation.

In this work, we seek to better understand and constrain the relative contributions of different creep mechanisms on the effective viscosity of glacier ice. We apply the composite flow law (Equation 3) to illuminate the partitioning of deformation rate between the two dominant creep mechanisms: dislocation creep and grain-boundary sliding. In doing so, we evaluate the controls that the rheological parameters (the prefactor and activation energy in the flow-rate parameters) have on this partitioning, with specific focus on the effect of activation energy.

ESTIMATING THE EFFECTS OF RHEOLOGICAL PARAMETERS ON THE DOMINANT DEFORMATION MECHANISM

From the composite flow law, we define γ to be the fraction of the overall deformation rate attributable to deformation by dislocation creep such that

$$\gamma = \frac{\dot{\epsilon}_{\text{dis}}}{\dot{\epsilon}} = \frac{A_{\text{dis}}\tau_e^{n_{\text{dis}}}}{\dot{\epsilon}} \tag{5}$$

where $n_{\text{dis}} = 4$ is the stress exponent for dislocation creep. By extension, the fraction of deformation rate attributable to grain-boundary sliding is $(1-\gamma)$. Direct estimates of γ can provide insight into the partitioning between mechanisms of deformation, which can inform studies into the controls on ice flow.

To estimate γ, we solve for ice temperature T, grain size d, and stress τ_e with a coupled model, given an observed total rate of deformation $\dot{\epsilon} = \dot{\epsilon}_{\text{obs}}$:

$$T = T(\dot{\epsilon}_{\text{obs}}, a, H) \tag{6a}$$

$$d = d(\dot{\epsilon}_{\text{obs}}, T) \tag{6b}$$

$$\tau_e = \tau_e(T, d, \dot{\epsilon}_{\text{obs}}) \tag{6c}$$

where a is surface mass balance and H is ice thickness. We find ice temperature T using the thermomechanical model – which includes advection, diffusion, and heating from viscous dissipation – derived by Meyer and Minchew (2018) and we find grain size d using the steady-state grain size model derived by Ranganathan and others (2021). We find τ_e from the composite flow law (Equation 3b) using a nonlinear equation solver. We then plug T, τ_e and d into Equation 5 to find the fraction of dislocation creep for an observed overall deformation rate $\dot{\epsilon}$.

EVALUATING THE EFFECT OF UNCERTAINTIES IN RHEOLOGICAL PARAMETERS ON ESTIMATED DEFORMATION MECHANISM

The focus of this study is to consider the effects of rheological parameters (the prefactor and activation energy in the flow-rate parameter) on this partitioning between deformation mechanisms (γ). In total, we consider eight parameters: the prefactor and the activation energy for low-temperature dislocation creep, high-temperature dislocation creep, low-temperature grain-boundary sliding, and high-temperature grain-boundary sliding. To evaluate the effects of uncertainties in these parameters, we use existing values of rheological parameters found in experimental studies (compiled by and cited in Zeitz and others (2021)) to define probability distributions by the means and standard deviations of these distributions.

We assume that activation energies vary along a normal distribution about the laboratory values presented in Table 1, from Goldsby and Kohlstedt (2001) and Kuiper and others (2020a). We assume a normal distribution because there are not enough datapoints to define a distribution with any certainty from existing observations. Based on the spread in estimates from experiments, we define a standard deviation of 10^4 J mol^{-1}. The prefactors in the flow-rate parameter have fewer estimated values and therefore, to test a variation in these parameters of orders of magnitude, we assume uncertainties in the prefactors can be

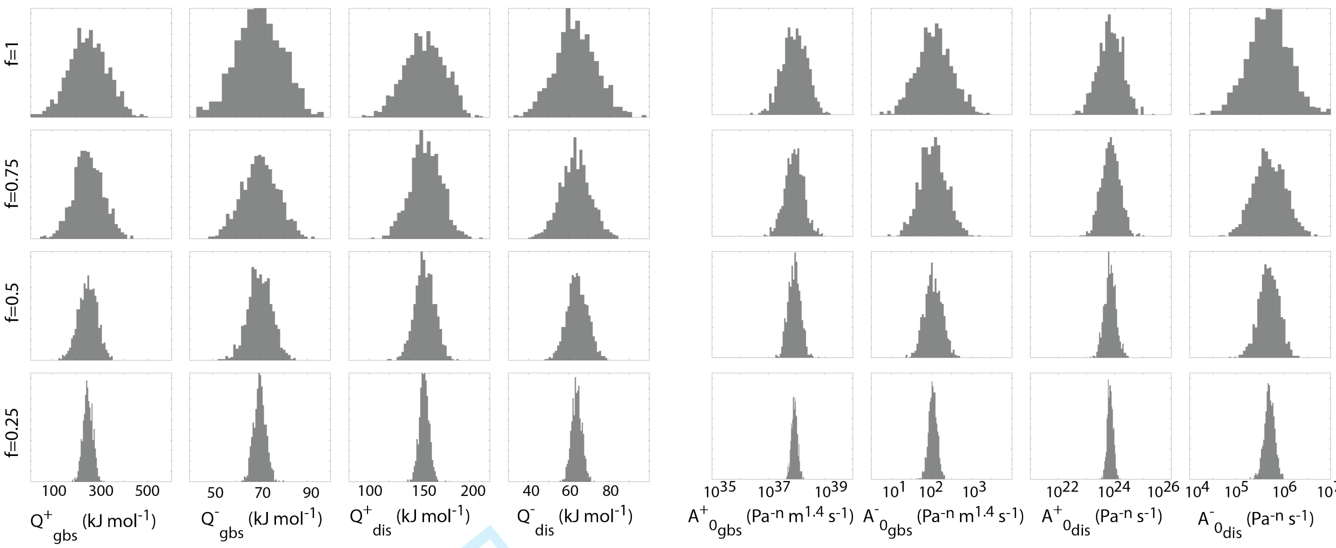

Fig. 1. Prior distributions of flow-rate parameter prefactors and activation energies: Normal distributions of the activation energies of the flow-rate parameters for grain-boundary sliding at high temperatures (first column) and low temperatures (second column) and of the activation energies of the flow-rate parameters for dislocation creep at high temperatures (third column) and low temperatures (fourth column). Log-normal distributions of the prefactors of the flow-rate parameters for grain-boundary sliding at high temperatures (fifth column) and low temperatures (sixth column) and of the prefactors of the flow-rate parameters for dislocation creep at high temperatures (seventh column) and low temperatures (eighth column). Standard deviations are multiplied by a factor f that varies from $f = 1$ to $f = 0.25$ (rows) as a way of exploring the uncertainties.

approximated as a log-normal distribution, with a standard deviation of one order of magnitude. One order of magnitude represents the maximum rheological effect of fabric (Cuffey and Paterson, 2010; Hudleston, 2015; Minchew and others, 2018), meaning the uncertainties we explore account for fabric if we assume that ice is in a fixed flow regime (so that anisotropy caused by faric can be represented as an enhancement multiplier to a scalar prefactor A) and fabric does not alter activation energy or the stress exponent n. We set the same standard deviation for all the activation energies and the same standard deviation for all the prefactors, as we have no present evidence to suggest that some of the parameters are less uncertain than the others. The means of these distributions are found in Table 1.

To test the effect that the magnitude of uncertainty has on γ estimates, we consider different levels of uncertainty. To do so, we define a multiplicative factor $f = 1, 0.75, 5, 0.25$ which we apply to the standard deviation of the distributions. Decreasing value of f reduces the standard deviation in the distributions (as a way of approximating a reduction in the uncertainty of the parameter). The resulting eight distributions for varying f can be seen in Figures 1, in which we show an ensembles of 1000 members drawn from the distributions defined above. These are the prior distributions of the rheological parameters.

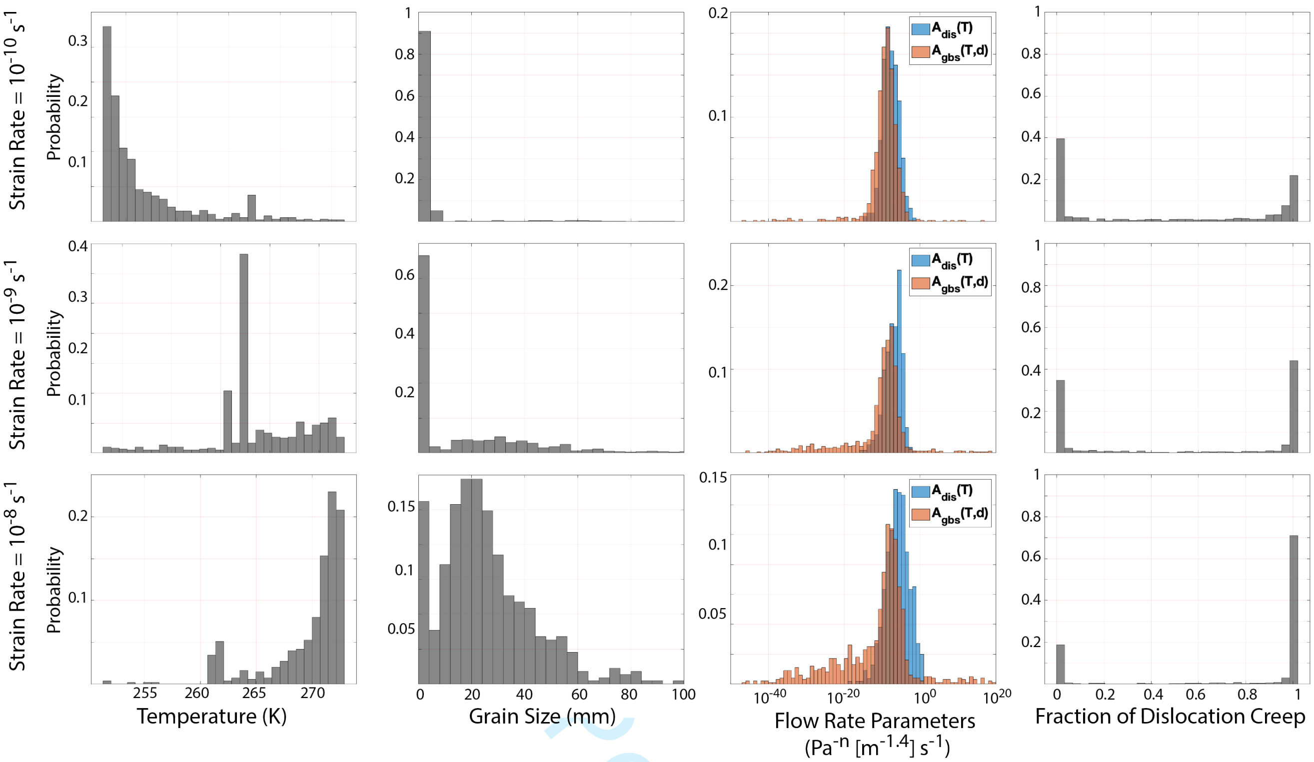

Fig. 2. Posterior distributions of γ, the fraction of dislocation creep: Ensembles of ice temperature (first column), grain size (second column), flow-rate parameters for dislocation creep and grain-boundary sliding (third column), and fraction of dislocation creep γ (fourth column), estimated from ensembles of the prefactors and activation energies shown in Figure 1. Here, we use $f = 1$, the maximum uncertainty. These are shown for three different strain rates (rows).

Estimating probabilities of γ from prior distributions of A_0, Q

We initially let $f = 1$ for all eight parameters, representing the maximum uncertainty, and we visualize how uncertainties in the flow parameters translate to uncertainties in estimates of ice temperature, grain size, and the fraction of dislocation creep γ. We define an ensemble for each flow parameter with 500 members, drawn from the distributions shown in Figure 1 (top row), and we input those ensembles into the temperature model, grain size model, and Equation 3b to estimate γ. Figure 2 shows the resulting distributions for three strain rates the represent those found in extant glaciers and ice sheets.

For low strain rates ($\dot{\epsilon} = 10^{-10}$ s^{-1}), the distribution of temperatures is skewed, with most ensemble members falling < 255 K and very few ensemble members falling > 262 K. For intermediate strain rates ($\dot{\epsilon} = 10^{-9}$ s^{-1}), the temperature distribution shifts towards larger temperatures, with most of the ensemble members at high temperatures (> 262 K). For larger strain rates ($\dot{\epsilon} = 10^{-8}$ s^{-1})), most of the density of the temperature distribution is > 262 K.

Estimates of grain size have a strong temperature dependence due to the kinetics of recrystallization processes (Ranganathan and others, 2021). At low temperatures ($T \leqslant 262$ K), grain sizes are $\sim 1-5$ mm, whereas at high temperatures ($262 < T \leqslant 273$ K), the bulk of the grain size distribution is $\sim 10-30$ mm. The strong dependence on ice temperature occurs due to the abrupt increase in activation energy and prefactor for creep and grain-boundary mobility at $T = 262$ K (Duval, 1981; Derby and Ashby, 1987; Duval and Castelnau, 1995; Urai and others, 1995; Alley, 1992; Jacka and Li Jun, 1994; Dash and others, 2006). This process results in larger grain sizes, which models suggest tend to be found in regions of high stresses and high temperatures (Ranganathan and others, 2021). The estimates of grain size shown here are larger than the average grain sizes seen in many glaciers, including smaller temperate glaciers where one might expect coarser grains (Gerbi and others, 2021). However, grain sizes of > 20 mm have been seen in some temperate glaciers (Tison and Hubbard, 2000) and in the basal regions of ice sheets (Gow and others, 1997; Thorsteinsson and others, 1997).

Besides estimated stresses, the key control on the fraction of dislocation creep is the balance between $A_{\text{dis}}(T)$ and $A_{\text{gbs}}(T, d)$. For low strain rates, both distributions roughly overlap, suggesting that, for similar magnitudes of stresses, neither term in the composite flow law (Equation 3b) would be significantly larger than the other. As strain rates increase, the distribution for $A_{\text{gbs}}(T, d)$ moves to lower values, while the distribution for $A_{\text{dis}}(T)$ moves to higher values.

This affects estimates of γ. In general, for all strain rates, there is very little density at intermediate values of γ ($0.2 < \gamma < 0.8$). This implies that there is a low probability of "composite flow", in which both dislocation creep and grain-boundary sliding are important contributors to the bulk deformation and $n \approx 3$. For low strain rates (10^{-10} s^{-1}), the probabilities of small $\gamma \approx 0.2$ and probabilities of large $\gamma \approx 0.35$, suggesting that grain-boundary sliding ($n \approx 2$) accounts for the majority of deformation. At higher strain rates, the probability of large γ increases and the probability of small γ decreases, suggesting that dislocation creep ($n = 4$) becomes the dominant creep mechanism.

Determining the controls of $p(\gamma)$

Estimating a posterior distribution of γ suggests a framework for determining the probability of either mechanism (dislocation creep or grain-boundary sliding) being the dominant flow mechanism for given flow conditions. This involves looking at the posterior distributions of γ and determining the number of ensemble members at high γ, which will tell us the probability of dislocation creep being dominant, and determining the number of ensemble members at low γ, which will tell us the probability of grain-boundary sliding being dominant. However, this requires us to define a threshold γ_t where $\gamma > \gamma_t$ suggests dislocation creep is dominant ($n = 4$), and $\gamma < 1 - \gamma_t$ we can assume that grain-boundary sliding is dominant ($n = 2$). For values $1 - \gamma_t \leqslant \gamma \leqslant \gamma_t$, we assume that the ice is flowing by composite flow, a combination of the two mechanisms ($n \approx 3$). Here, we let the threshold $\gamma_t = 0.75$, representing a value large enough that we can assume the flow is governed by dislocation creep, though we note that this specific choice in value is heuristic. We then define probabilities such that

$$\text{p(dislocation creep)} = \frac{\text{number of members with } \gamma > \gamma_t}{\text{number of total ensemble members}} \tag{7a}$$

$$\text{p(grain boundary sliding)} = \frac{\text{number of members with } \gamma < 1 - \gamma_t}{\text{number of total ensemble members}} \tag{7b}$$

$$\text{p(both)} = \frac{\text{number of members with } 1 - \gamma_t \leqslant \gamma \leqslant \gamma_t}{\text{number of total ensemble members}} \tag{7c}$$

To examine which flow parameters are controlling these probabilities, we vary f_{A_0} for the prefactors A_0 and f_Q for the activation energies Q separately and determine the probabilities of dislocation creep, grain-boundary sliding, and both as functions of f_A, f_Q (Figure 3).

The probabilities of dominant deformation mechanism are strongly dependent on f_Q (Figure 3; top row). Holding $f_{A_0} = 1$, we see that at high strain rates (10^{-8} s^{-1}), the probability of dislocation creep varies from $\sim 0.6 - 0.8$ for varying f_Q. There are low probabilities of grain-boundary sliding and both mechanisms acting together, and these probabilities change for varying f_Q. At low strain rates (10^{-10} s^{-1}), the probability of dislocation creep ~ 0.4 and probability of grain-boundary sliding ~ 0.5 at largest f_Q, and the probability of dislocation creep decreases to ~ 0.1 as f_Q decreases, while the probabilities of both and grain-boundary sliding increase or remain the same.

When we widen the prefactor distributions only (changing f_{A_0} while holding $f_Q = 1$) the probability of dislocation creep, probability of grain-boundary sliding, and probability of both do not significantly change with varying f_{A_0} (Figure 3; bottom row), suggesting that uncertainties in the prefactors of the flow-rate parameters do not significantly affect uncertainties in γ. By extension, this suggests that the development of fabric will not alter the balance of creep mechanisms nor the value of the stress exponent n. The probability of dislocation creep is high for high strain rates (p(dislocation creep) $\approx 0.7 - 0.8$) and decreases for decreasing strain-rate. At lowest strain rate (10^{-10} s^{-1}), the probability of grain-boundary

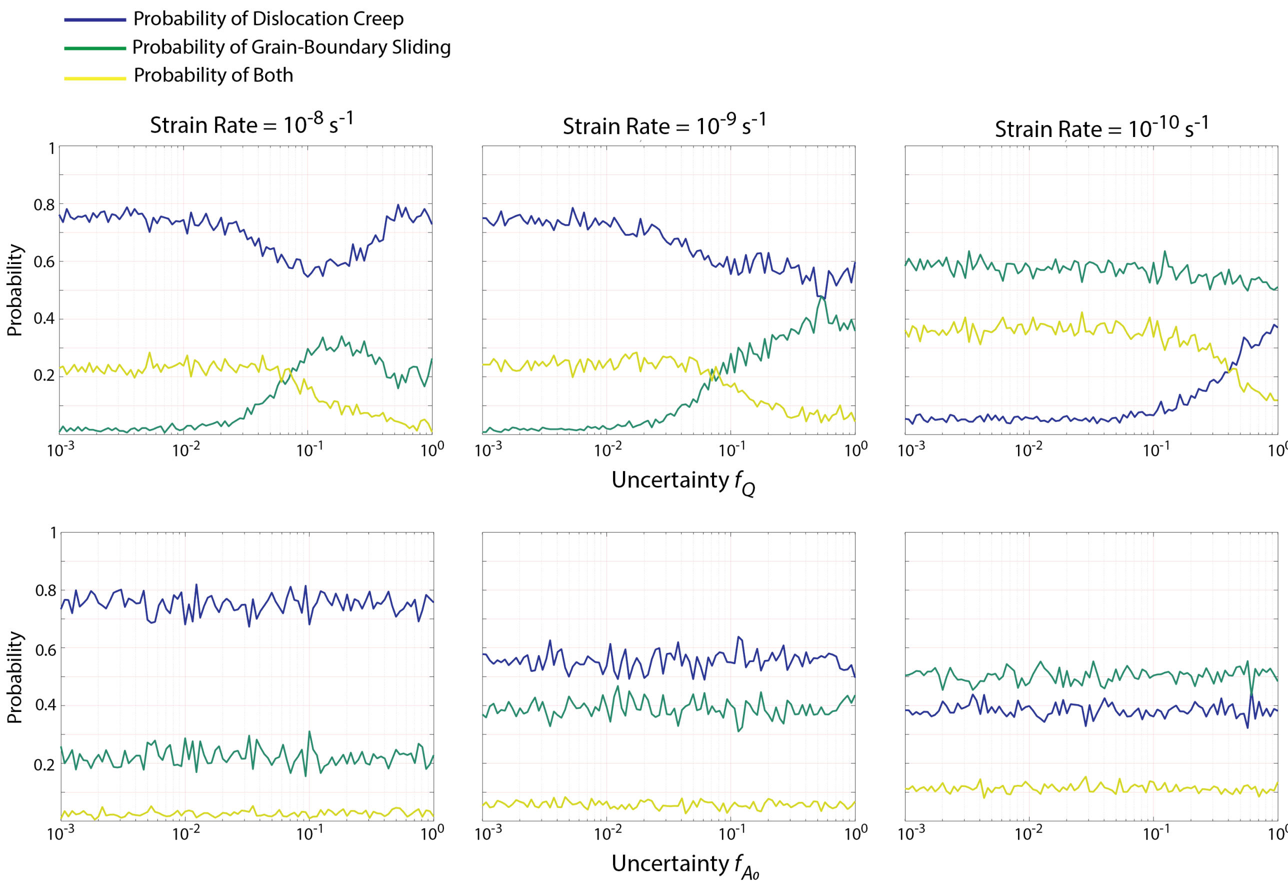

Fig. 3. Probable balance of creep mechanisms for varying prefactor and activation energy uncertainties: Probability of dislocation creep ($n = 4$), grain-boundary sliding ($n = 2$), and both ($n \approx 3$) for varying activation energy uncertainty (top row) and prefactor uncertainty (bottom row). This is shown for three different strain-rates. Note that it is rarely the case that both mechanisms contributing in important ways is the most probable scenario, meaning that $n = 3$ is not the most likely value of the stress exponent n in our analysis.

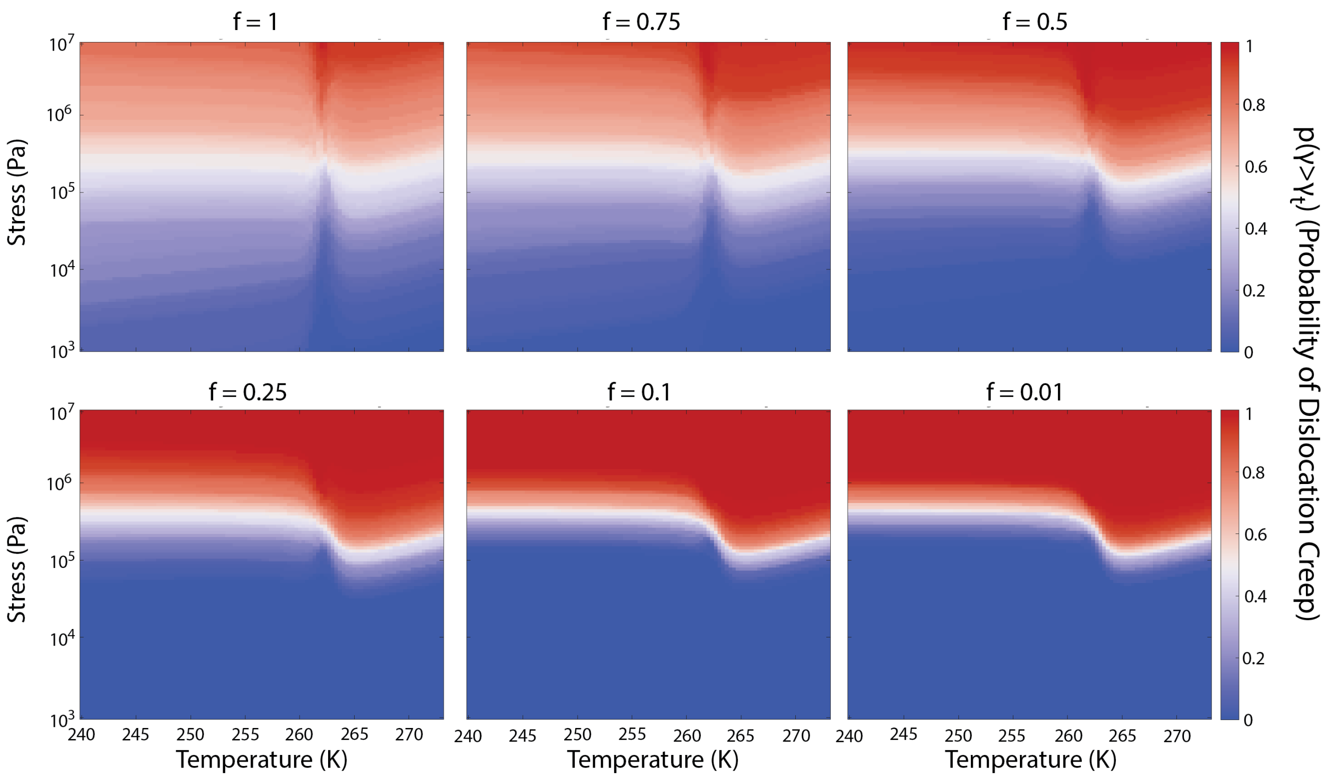

Fig. 4. Probabilities of γ for varying uncertainty in activation energy: Estimates of the probability of dislocation creep dominating ($p(\gamma > 0.75)$) for: $f_Q = 1$, $f_Q = 0.75$, $f_Q = 0.5$, $f_Q = 0.25$, $f_Q = 0.1$, $f_Q = 0.01$.

sliding is larger than the probability of dislocation creep.

For a more complete examination, we calculate $p(\gamma > \gamma_t)$, the probability of dislocation creep being dominant (*i.e.*, the probability of $n = 4$ in Glen's Flow Law), for a range of temperatures common to ice sheets and glaciers ($240 - 273$ K) and a wide range of stresses ($10^3 - 10^7$ Pa) (Figure 4). For all values of f, the probability of dislocation creep is high for higher stresses ($>$ 100 kPa) and low for low stresses ($<$ 10 kPa), suggesting that at stresses above 100 kPa, dislocation creep is very likely to be the dominant deformation mechanism and at stresses below 10 kPa, grain-boundary sliding is likely to be the dominant deformation mechanism.

However, the stress dependence varies with ice temperature. At high temperatures ($262 \leqslant T \leqslant 273$ K), dislocation creep dominates for lower stresses due to the effect of temperature on $A_{\rm dis}$ and $A_{\rm gbs}$. The increase of p(dislocation creep) with increasing temperature arises from both increasing temperature and increasing grain-size. Since the contribution of grain-boundary sliding to overall deformation rate is inversely dependent on grain size, regions of large grain sizes will tend to deform by dislocation creep primarily. The structure and magnitude of this increase in p(dislocation creep) therefore depends on the grain-size model used. There is a boundary between $10 - 100$ kPa for which the probabilities of dislocation creep and grain-boundary sliding dominating are roughly equal. As shown in the Supplement, there remains a very low probability of $n \approx 3$ where ice deforms due to dislocation creep and grain-boundary sliding acting in approximately the same proportions (*i.e.*, $\dot{\epsilon}_{gbs} \sim \dot{\epsilon}_{dis}$).

Uncertainties in the activation energies for creep also affect these probabilities. For very low uncertainties ($f = 0.01$), the boundary in which p(dislocation creep) (as defined by Equation 7a) is $0.2 - 0.8$ lies between $10 - 100$ kPa. This boundary widens with increasing uncertainty. At the maximum uncertainty ($f = 1$), p(dislocation creep) > 0.8 is only true for stresses greater than ~ 500 kPa. The same is shown to be true with respect to grain-boundary sliding: increasing uncertainty reduces the range of stresses for which grain-boundary sliding is very likely (with probability > 0.8) to be the dominant mechanism.

While here we look at a wide range of stresses, the stresses most common in the fast-flowing regions of glaciers and ice sheets are generally $\sim 10 - 1000$ kPa. Notably, this range encompasses the boundary between p(dislocation creep) ≈ 1 and p(dislocation creep) ≈ 0 even at the lowest uncertainty ($f = 0.01$), suggesting that for the stresses most applicable to glaciers and ice sheets, the dominant deformation mechanism is sensitive to ice temperature and other conditions besides stress, which are accounted for through the flow-rate parameters A_{dis} and A_{gbs}. This highlights the importance of evaluating the uncertainties and calibrated values of activation energy, the models we use for ice temperature and grain size, and the way we parameterize the flow-rate parameter.

VALUE OF ACTIVATION ENERGY

In the previous section, we evaluated the effect of the standard deviation about the laboratory values (Table 1) on our confidence in the deformation mechanism of ice flow. Here, we consider how altering the values of the activation energies in a deterministic framework may affect our estimates of the relative contributions of the deformation mechanisms.

Effect of Values of Activation Energy on γ and $p(\gamma)$

Given the significant uncertainties in the activation energy values and how these uncertainties affect estimates of ice flow, it is not presently clear how broadly applicable the laboratory values are to naturally-deforming ice. Therefore, here we consider the effect of altering the activation energy values in a deterministic framework on the estimated deformation mechanism. We calculate γ for varying grain-boundary sliding and dislocation creep activation energies, to determine the effect of different combinations of these

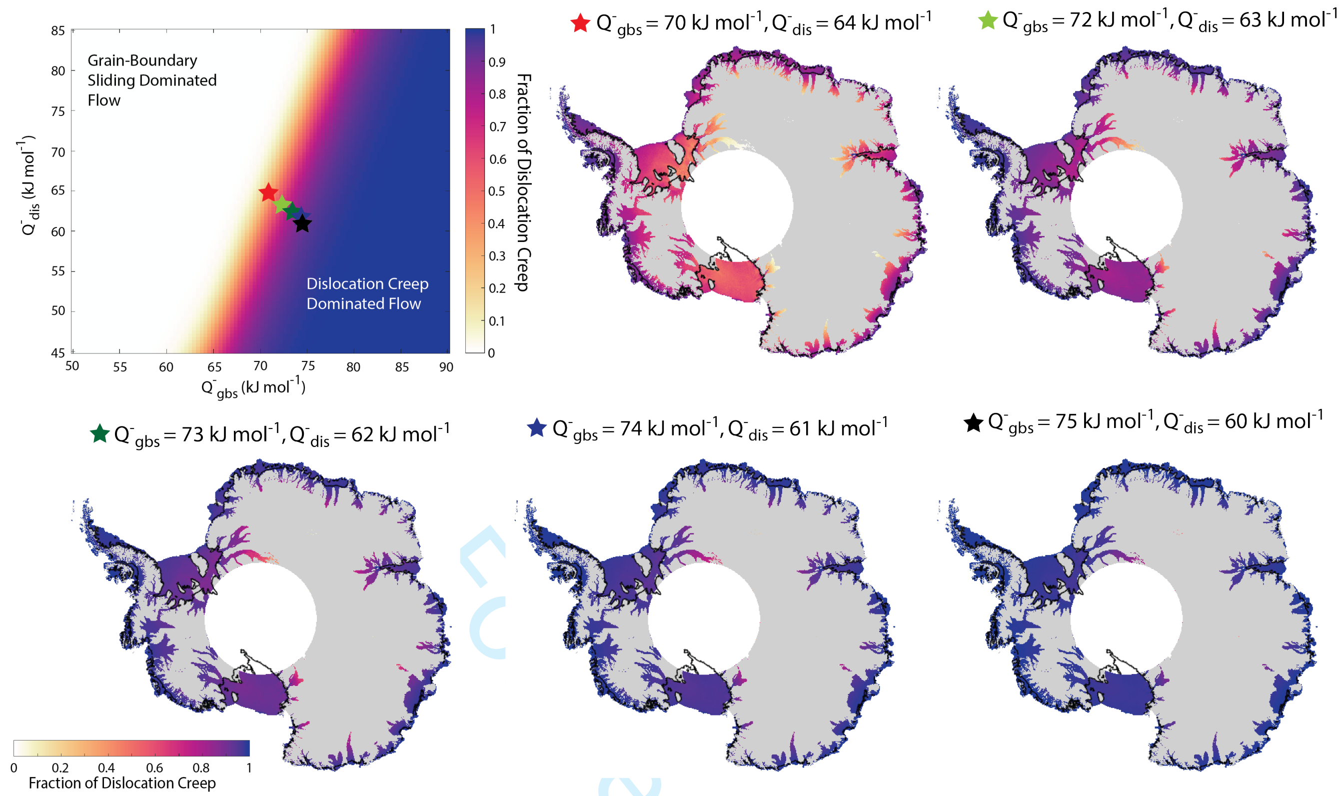

Fig. 5. Estimates of γ for varying activation energy values: We show 5 different activation energy scenarios (denoted by differently-colored stars on the upper-left hand plot of γ) and their impact on estimates of γ across the Antarctic Ice Sheet. Values given in Table 1 are denoted by the red star. Regions where surface velocity is less than 30 m a^{-1} are shown in grey, as our model is not applicable in these regions. For the plot in the upper left corner, we prescribe $\dot{\epsilon} = 10^{-10}$ s^{-1} and $T = 250$ K. For the Antarctica maps, we drive the model using observed strain rates (Meyer and Minchew, 2018), ice thicknesses (Howat and others, 2019; Morlighem and others, 2020), and surface temperature and mass balance from RACMO reanalysis data (Van Wessem and others, 2014). Other parameters are given in the respective publications (Meyer and Minchew, 2018; Ranganathan and others, 2021).

uncertain parameters. In this idealized set-up, we let $\dot{\epsilon}_e = 10^{-10}$ s^{-1} and $T = 250$ K, and therefore we only vary the low-temperature activation energy value (Figure 5; upper-left). The laboratory values are denoted by a red star, and different pairs of activation energies are shown by the remaining stars.

Estimates of deterministic γ vary significantly based on values of low-temperature activation energy. In general, γ is small for low values of $Q^-_{\rm gbs}$ and high values of $Q^-_{\rm dis}$ and γ is large for high values of $Q^-_{\rm gbs}$ and low values of $Q^-_{\rm dis}$. This is expected given the kinetics; when activation energies for dislocation creep are large, deformation by dislocation creep will be more difficult and therefore γ will be lower. Similarly, when activation energies for grain-boundary sliding are large, deformation by grain-boundary sliding will require more energy and therefore γ will be higher. There is a clear boundary between $\gamma \approx 0$ and $\gamma \approx 1$, in which $0.2 < \gamma < 0.8$ for some combinations of $Q^-_{\rm gbs}$ and $Q^-_{\rm dis}$.

The laboratory values of low-temperature activation energies lie on one edge of this boundary, suggesting that, at the strain-rate and temperature in which we conduct this study, $\gamma \approx 0.2 - 0.3$. This would imply that under these flow conditions, ice deformation likely occurs predominantly by grain-boundary sliding. We examine other calibrations of activation energies that lie along the rest of this boundary, which represent very small deviations from the laboratory values (of < 5 kJ mol^{-1}). In this idealized set-up, these other calibrations produces significantly different γ estimates, ranging from $\gamma \approx 0.2$ to $\gamma \approx 0.9$.

Using observed strain-rates, we can estimate γ over the Antarctic Ice Sheet using these varying calibrations of activation energies. To do this, we use strain-rates derived from Landsat 7 and 8 surface velocity observations (Gardner and others, 2018; Alley and others, 2018), ice thickness found from the Reference Elevation Model of Antarctica and BedMachine (Howat and others, 2019; Morlighem and others, 2020), and surface temperature and mass balance from RACMO (Van Wessem and others, 2014). We solve for γ using Equation 5 over the fast-flowing regions of the Antarctic Ice Sheet (those with velocities > 30 m a^{-1}). For regions of high-temperature flow, we make the same adjustments to high-temperature activation energies that we do to the low-temperature activation energies, to preserve the relative balance between the two.

For the laboratory values of the parameters (red star), we estimate $\gamma > 0.7$ for most of the rapidly-deforming regions. This encompasses most areas on the margin of the ice sheet and in the margins of the ice streams. We estimate $\gamma < 0.4$ for only slower-flowing regions, such as the upper regions of ice streams. We estimate $\gamma \approx 0.5 - 0.6$ on the major ice shelves, suggesting roughly equal contributions from dislocation creep and grain-boundary sliding. Dislocation creep appears to dominate for much of the most dynamic, grounded regions of the ice sheet.

However, the estimates of γ increase significantly with minor changes to the activation energy values. For $\Delta Q^{-}_{\text{gbs}} = 2$ kJ mol^{-1} and $\Delta Q^{-}_{\text{dis}} = -1$ kJ mol^{-1}, $\gamma \approx 1$ along many of the rapidly-deforming ice streams (such as Pine Island Glacier) and $\gamma \approx 0.8$ on the ice shelves, suggesting that dislocation creep dominates along most of the fast-flowing regions of the ice sheet. γ remains low only for the most upstream portions of a few ice streams, such as Recovery Ice Stream. As Q^{-}_{gbs} increases and Q^{-}_{dis} decreases, $\gamma \to 1$ for all of the fast-flowing regions of the ice sheet. The final recalibration we consider, with $Q^{-}_{\text{gbs}} = 75$ kJ mol^{-1} and $Q^{-}_{\text{dis}} = 60$ kJ mol^{-1}, lies on the other end of the boundary between $\gamma \approx 0$ and $\gamma \approx 1$ in the figure of varying low-temperature activation energies. At these activation energy values, $\gamma = 1$ on all fast-flowing ice streams and ice shelves, suggesting that dislocation creep dominates ice flow on the Antarctic Ice Sheet.

We can do a similar study of the effect of recalibrations of activation energy in a probabilistic framework,

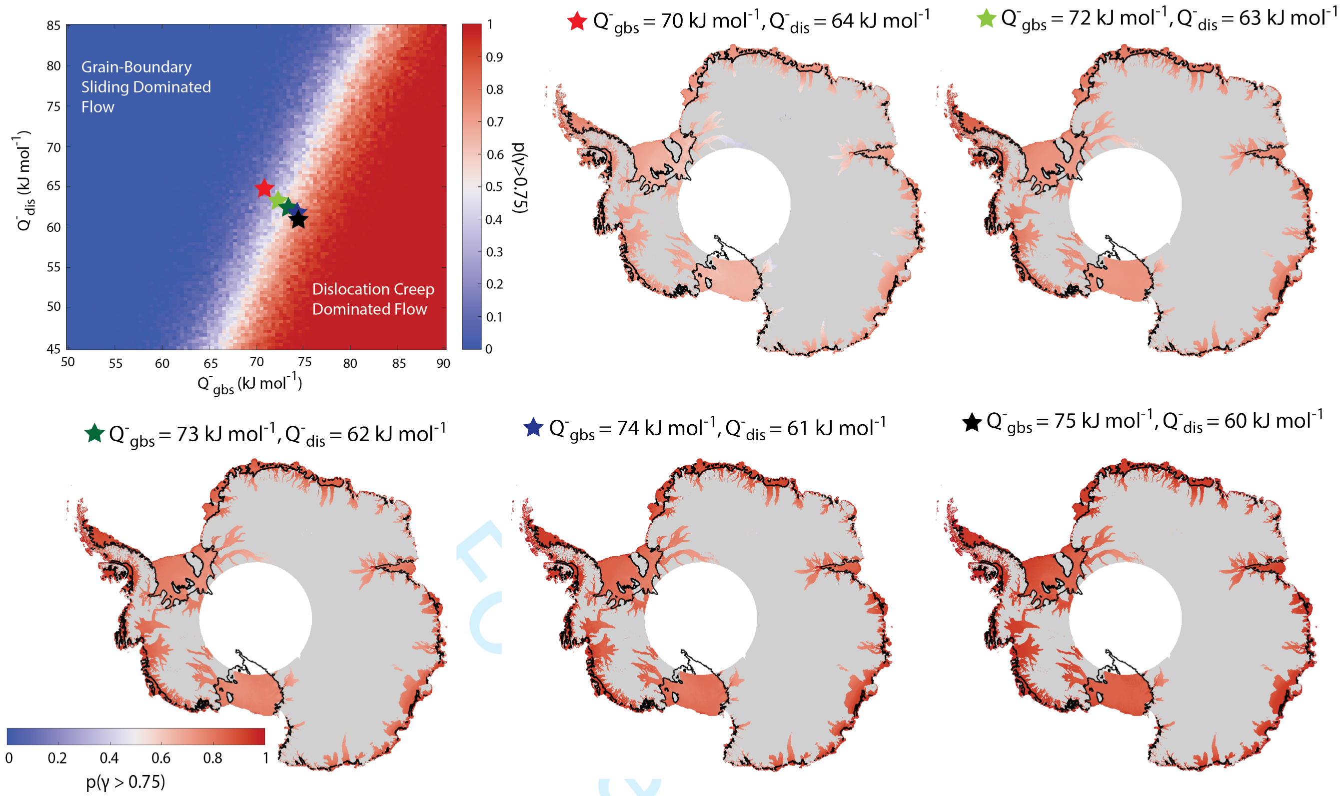

Fig. 6. Estimates of p(dislocation creep) for varying activation energy values: We show 5 different activation energy scenarios (denoted by differently-colored stars on the upper-left hand plot of probability of $\gamma > 0.75$) and their impact on estimates of $p(n \geqslant 3.5)$ across the Antarctic Ice Sheet. The star colors are the same as in Figure 5 as are the data sets used to drive the models and the temperature and strain rate for the upper left plot. Regions where surface velocity is less than 30 m a^{-1} are shown in grey, as our model is not applicable in these regions.

accounting for uncertainty in the distribution and altering the means of the distributions (Figure 6). Since we've set the standard deviation of the prior distributions to approximate the full range of values found by laboratory studies, when applying this framework to data we set $f = 0.5$ as a way of approximating a normal distribution in which two standard deviations captures the full range of values identified in laboratory studies. We set the prefactor to be deterministic, using the laboratory values as shown in Table 1.

For varying low-temperature activation energies for dislocation creep and grain-boundary sliding, we compute the probability of dislocation creep being dominant ($p(\gamma > 0.75)$) and find a similar structure as in Figure 5. The probability of dislocation creep being dominant is very low for high Q^{-}_{dis}, low Q^{-}_{gbs} and is very high for low Q^{-}_{dis}, high Q^{-}_{gbs}. There is a boundary between the two regimes that encompasses the laboratory values of activation energy.

For laboratory values of the parameters and applying the same standard deviation to the activation energy distributions described in the previous section, the probability of dislocation creep being dominant is $\sim 0.5 - 0.6$ across most of the continent. The probability is slightly higher ($\sim 0.6 - 0.7$) in the rapidly-deforming regions, such as the margins of ice streams and in trunks of fast-flowing ice streams like Pine Island Glacier. The probability is lower ($\sim 0.4 - 0.5$) in slow-flowing regions, such as upstream of Recovery Ice Stream. These probabilities suggest that while dislocation creep may be estimated to be a larger contributor to overall strain-rate, the uncertainties in activation energy are large enough that we cannot present this result with a high degree of confidence. As we alter the activation energy values across the boundary, the probability of dislocation creep being dominant increases. At the other end of the boundary, with $Q^-_{\mathrm{gbs}} = 75$ kJ mol^{-1} and $Q^-_{\mathrm{dis}} = 60$ kJ mol^{-1}, the probability of dislocation creep being dominant is > 0.8 across most of the ice sheet, including in slower-flowing regions such as the centers of large ice shelves.

Using Observations to Recalibrate Activation Energies

Based on these results, the estimates of the dominant deformation mechanism, computed based on a composite flow law (Equation 3b), are quite sensitive to the values of activation energies for creep. Further, uncertainties in activation energy values translate to significant uncertainties in the estimates of dominant deformation mechanism. This has implications for how we model ice flow largely because the value of the stress exponent in Glen's Flow Law n is a representation of the deformation mechanism. If dislocation creep is dominant, it is likely that $n = 4$ is the appropriate value of the stress exponent, while when grain-boundary sliding is dominant, $n = 2$ is the most applicable integer. Therefore, uncertainties in the activation energy directly affect our confidence in the values we use when modeling ice flow.

Recently, remote sensing has provided ways of estimating n from observations, as done by Bons and others (2018) and Millstein and others (2022), which enables data-driven benchmarking of flow parameters. Both studies estimated the dependence of deformation rate on stress in slower-deforming, likely cold regions of ice sheets. Bons and others (2018) studied the northern, vertical shear-dominated regions of the Greenland Ice Sheet. Millstein and others (2022) considered the regions of Antarctic ice shelves dominated by extensional flow. These studies estimated that $n \approx 4$ (indicating that dislocation creep is dominant) in their study areas. This observation is inconsistent with the estimate of γ using laboratory values of activation energies, as shown in Figure 5. For low-temperature deformation at the laboratory values of activation energies, we find that $\gamma \approx 0.2$ (red star; Figure 5), implying that $n \approx 2$. We propose that this

Table 2. Rheological parameters for dislocation creep and grain-boundary sliding, recalibrated based on observations (Bons and others, 2018; Millstein and others, 2022).

Parameter	**Value**	**Unit**
$A^{+}_{0_{\rm dis}}$	6.96×10^{23}	$\mathrm{MPa}^{-\mathrm{n}_{\mathrm{dis}}}\ \mathrm{s}^{-1}$
$A^{-}_{0_{\rm dis}}$	5×10^{5}	$\mathrm{MPa}^{-\mathrm{n}_{\mathrm{dis}}}\ \mathrm{s}^{-1}$
$Q^{+}_{\rm dis}$	151×10^{3}	$\mathrm{J\ mol}^{-1}$
$Q^{-}_{\rm dis}$	60×10^{3}	$\mathrm{J\ mol}^{-1}$
$A^{+}_{0_{\rm gbs}}$	8.5×10^{37}	$\mathrm{MPa}^{-\mathrm{n}_{\mathrm{gbs}}}\ \mathrm{m}^{m}\ \mathrm{s}^{-1}$
$A^{-}_{0_{\rm gbs}}$	1.1×10^{2}	$\mathrm{MPa}^{-\mathrm{n}_{\mathrm{gbs}}}\ \mathrm{m}^{m}\ \mathrm{s}^{-1}$
$Q^{+}_{\rm gbs}$	255×10^{3}	$\mathrm{J\ mol}^{-1}$
$Q^{-}_{\rm gbs}$	75×10^{3}	$\mathrm{J\ mol}^{-1}$

inconsistency may come from the values of activation energy used in this model, given that γ is extremely sensitive to the activation energies and less sensitive to other parameters in the composite flow law, such as the prefactor. Further, there is a significant range of activation energies found by experimental studies, and therefore the laboratory values may not necessarily be the most accurate parameters to apply to ice deformation.

To ensure consistency with observations, we propose a recalibration of the low-temperature activation energy values to calculate $\gamma \approx 1$ in conditions similar to those studied in Bons and others (2018) and Millstein and others (2022), while minimizing deviations from the laboratory values. We choose $Q^{-}_{\rm gbs} = 75$ kJ mol^{-1} and $Q^{-}_{\rm dis} = 60$ kJ mol^{-1}, values well within the range of laboratory experiments (Zeitz and others, 2021, and references therein) and denoted by black stars in Figs 5 and 6. We recalibrate the high-temperature activation energy values to preserve the relative behaviors in low- and high-temperature deformation. For practical purposes, this means that we adjust the high-temperature values to provide a smooth transition in strain rate in the vicinity of temperature transition from warm to cold activation energies. The recalibrated parameters are fully presented in Table 2.

There is a possibility that the inconsistency between observations and our model estimates with the laboratory values comes from some other process not accounted for in this model. If this inconsistency is due to simplifications of the model itself, the calibration of these activation energy values could be thought of as a parameterization of these processes not captured in the model, in a similar way that we parameterize the strain-rate acceleration at high temperatures by a discontinuous increase in activation energy (Cuffey and Paterson, 2010).

DISCUSSION AND CONCLUSION

In this study, we consider the effect of activation energy on ice deformation. Activation energy enters into the representation of ice deformation through the flow-rate parameters in the constitutive relation relating stress and strain rate, and governs the temperature dependence of ice viscosity. Therefore, activation energies have an outsized effect on ice flow.

Here, we apply a composite flow law as presented in Goldsby and Kohlstedt (2001) to determine the partitioning of the total strain rate between two ice deformation mechanisms, dislocation creep and grain boundary sliding, by defining γ as the fraction of dislocation creep. We examine the effect of the values and uncertainties in activation energy on our estimates of γ.

We find first that activation energy has a significant effect on estimates of γ, while the prefactors in the flow-rate parameter do not. The latter indicates that the presence of crystallographic preferred orientation, or fabric, which would alter the prefactor and not the activation energy, does not influence the relative contributions of creep mechanisms nor the value of the stress exponent n. Further, we find that, using the laboratory values as means of a distribution and applying varying standard deviations, the probability of dislocation creep being the dominant deformation mechanism is very high for high stresses (> 1000 kPa) and very low for lower stresses (< 10 kPa). Between $10 - 1000$ kPa, the probability of dislocation creep dominating the flow varies significantly with the uncertainties in activation energy. Since these are stresses under which ice sheets and glaciers typically deform, this highlights the need to further constrain the activation energies for both dislocation creep and grain-boundary sliding.

We examine the specific values of activation energy used in ice flow models and find that small deviations from the laboratory values can produce large differences in estimates of the dominant deformation mechanism. In particular, deviations of $\leqslant 5$ kJ mol^{-1} can change γ from $\gamma \approx 0.3 - 0.4$ to $\gamma \approx 1$ in certain regions of the Antarctic Ice Sheet. We propose one way of constraining the values of activation energy may be to compare estimates of γ for varying activation energy values to estimates of n made by previous studies in naturally-deforming regions of ice sheets. In particular, we apply studies that have estimated $n = 4$ (suggesting dislocation creep is the dominant flow mechanism) in slower-deforming regions of ice sheets (Bons and others, 2018; Millstein and others, 2022) and find that values of low-temperature activation energies of $Q^{-}_{\mathrm{gbs}} = 75$ kJ mol^{-1} and $Q^{-}_{\mathrm{dis}} = 60$ kJ mol^{-1} (with the same magnitudes of changes made to the respective high-temperature activation energy values) produce a high probability of dislocation creep dominating in the regions of study by Bons and others (2018) and Millstein and others (2022). This suggests that, moving forward in ice flow modeling, we ought to further benchmark our values of activation energy with available observations and recalibrated activation energy values.

These results depend strongly on some key simplifications about ice flow. Primarily, they depend on the assumption that dislocation creep and grain-boundary sliding are both active in ice sheets, that the contributions of these two mechanisms operate independently such that their contributions can be summed according to the composite flow law, and that they are the dominant two mechanisms controlling ice flow in natural conditions. Some studies have suggested that the behavior identified by Goldsby and Kohlstedt (1997a, 2001) as grain-boundary sliding may in fact be descriptive of other processes, such as the accommodation of basal slip by grain-boundary migration, which acts as a recovery mechanism (Duval and others, 2000; Duval and Montagnat, 2002). While more work needs to be done to determine the physical mechanism behind the $n = 1.8$ regime, the analysis here is interested primarily in determining under which conditions each regime is most applicable, which uses the empirical values found by Goldsby and Kohlstedt (2001) and is not necessarily dependent upon precise descriptions of the mechanisms responsible for these values. However, uncertainties would be reduced by further investigation into which process is dominant and the incorporation of a physical understanding of that process into the model.

Because we focus on the prevalent stresses and temperatures found in existing glaciers and ice sheets, this work does not account for other creep mechanisms such as diffusion creep and basal slip, as well as more complex subsets of flow mechanisms, which all likely carry their own dependencies on ice temperature, grain size, and stress. Further, while this study has considered any mechanism at high stresses to be dislocation creep, the composite flow law used here primarily describes dislocation slip on basal planes. This neglects processes that have been identified to be active at high stresses, such as dislocation climb and slip that occurs on non-basal planes (Montagnat and Duval, 2004). While Goldsby and Kohlstedt (2001) suggests that mechanisms like diffusion creep and basal slip are unlikely to be dominant in naturally deforming ice, more work needs to be done to determine whether we can neglect these mechanisms and still accurately capture ice flow in our models.

There are still other processes, such as the development of a liquid phase at high temperatures (Duval, 1977; de La Chapelle and others, 1995; Wilson and Zhang, 1996; Wilson and others, 1996; De La Chapelle and others, 1999; Adams and others, 2021), that are not explicitly considered in this study. This effect may be parameterized within the abrupt change in flow law parameters (prefactor and activation energy in the flow-rate parameter) between high- and low-temperature deformation, as we have done in this study. The exact mechanism for this acceleration is poorly understood and may not, in fact, be due to a change in the flow parameters (Barnes and others, 1971; Jones and Brunet, 1978; Kuiper and others, 2020a). While here we follow the convention of the field and adopt empirical values of these parameters, this work suggests the need to further understand the kinetics of creep and the physical mechanisms controlling flow at high temperatures.

While we neglect some of the complexity of ice flow, we believe this study is a step towards understanding the controls of ice flow and identifying the parameters in ice flow models that ought to be further constrained. Further complexity in ice flow could be incorporated into this framework by altering the composite flow law used. Finally, estimates of γ could be used to calibrate the flow parameters, such as the stress exponent n, that ought to be used in ice flow models.

ACKNOWLEDGEMENTS

M.I.R. was supported by the School of Science Service Fellowship, Martin Fellowship, NSFGEO-NERC award 1853918, NEC Corporation Fund for Research in Computers and Communications, and the NOAA Climate & Global Change postdoctoral fellowship. B.M. acknowledges funding from NSFGEO-NERC award 1853918, NSF-NERC award 1739031, and NEC Corporation Fund for Research in Computers and Communications. The authors benefited greatly from discussions with Joanna Millstein, David Goldsby, Colin R. Meyer, Jerome Neufeld.

DATA STATEMENT

The source code for the model presented in this study are openly available at `https://github.com/megr090/ActivationEnergyUncertainties`. No new data were produced for this study, and data used in this study are publicly available through their respective publications.

REFERENCES

Adams CJC, Iverson NR, Helanow C, Zoet LK and Bate CE (2021) Softening of Temperate Ice by Interstitial Water. *Frontiers in Earth Science*, **9**(July), 1–11, ISSN 2296-6463 (doi: 10.3389/feart.2021.702761)

Alley KE, Scambos TA, Anderson RS, Rajaram H, Pope A and Haran TM (2018) Continent-wide estimates of Antarctic strain rates from Landsat 8-derived velocity grids. *Journal of Glaciology*, **64**(244), 321–332, ISSN 00221430 (doi: 10.1017/jog.2018.23)

Alley R (1992) Flow-law hypotheses for ice-sheet modeling. *Journal of Glaciology*, **38**(129), 245–256, ISSN 0022-1430 (doi: 10.3189/S0022143000003658)

Barnes P, Tabor D and Walker JCF (1971) The friction and creep of polycrystalline ice. *Proceedings of the Royal Society of London. A. Mathematical and Physical Sciences*, **324**(1557), 127–155, ISSN 2053-9169 (doi: 10.1098/rspa.1971.0132)

Bons PD, Kleiner T, Llorens MG, Prior DJ, Sachau T, Weikusat I and Jansen D (2018) Greenland Ice Sheet: Higher Nonlinearity of Ice Flow Significantly Reduces Estimated Basal Motion. *Geophysical Research Letters*, **45**(13), 6542–6548, ISSN 19448007 (doi: 10.1029/2018GL078356)

Budd W and Jacka T (1989) A review of ice rheology for ice sheet modelling. *Cold Regions Science and Technology*, **16**(2), 107–144, ISSN 0165232X (doi: 10.1016/0165-232X(89)90014-1)

Cuffey K and Paterson W (2010) *The Physics of Glaciers*. Elsevier, fourth edition

Dash JG, Rempel AW and Wettlaufer JS (2006) The physics of premelted ice and its geophysical consequences. *Reviews of Modern Physics*, **78**(3), 695–741, ISSN 15390756 (doi: 10.1103/RevModPhys.78.695)

de La Chapelle S, Duval P and Baudelet B (1995) Compressive creep of polycrystalline ice containing a liquid phase. *Scripta Metallurgica et Materialia*, **33**(3), 447–450, ISSN 0956716X (doi: 10.1016/0956-716X(95)00207-C)

De La Chapelle S, Milsch H, Castelnau O and Duval P (1999) Compressive creep of ice containing a liquid intergranular phase: Rate-controlling processes in the dislocation creep regime. *Geophysical Research Letters*, **26**(2), 251–254, ISSN 00948276 (doi: 10.1029/1998GL900289)

De Rydt J, Reese R, Paolo FS and Gudmundsson GH (2021) Drivers of Pine Island Glacier speed-up between 1996 and 2016. *The Cryosphere*, **15**(1), 113–132, ISSN 1994-0424 (doi: 10.5194/tc-15-113-2021)

Derby B and Ashby M (1987) On dynamic recrystallisation. *Scripta Metallurgica*, **21**(6), 879–884, ISSN 00369748 (doi: 10.1016/0036-9748(87)90341-3)

Duval P (1977) The role of the water content on the creep rate of polycrystalline ice. *IAHS Publ.*, **118**, 29–3332

Duval P (1981) Creep and Fabrics of Polycrystalline Ice Under Shear and Compression. *Journal of Glaciology*, **27**(95), 129–140

Duval P and Castelnau O (1995) Dynamic recrystallization of ice in polar ice sheets. *Journal de Physique IV*, **5**(C3), 197–205 (doi: 10.1051/jp4)

Duval P and Montagnat M (2002) Comment on "Superplastic deformation of ice: Experimental observations" by D. L. Goldsby and D. L. Kohlstedt. *Journal of Geophysical Research: Solid Earth*, **107**(B4), ECV 4–1–ECV 4–2, ISSN 01480227 (doi: 10.1029/2001JB000946)

Duval P, Ashby MF and Anderman I (1983) Rate-controlling processes in the creep of polycrystalline ice. *Journal of Physical Chemistry*, **87**(21), 4066–4074, ISSN 00223654 (doi: 10.1021/j100244a014)

Duval P, Arnaud L, Brissaud O, Montagnat M and de la Chapelle S (2000) Deformation and recrystallization processes of ice from polar ice sheets. *Annals of Glaciology*, **30**, 83–87, ISSN 0260-3055 (doi: 10.3189/172756400781820688)

Fan S, Hager TF, Prior DJ, Cross AJ, Goldsby DL, Qi C, Negrini M and Wheeler J (2020) Temperature and strain controls on ice deformation mechanisms: insights from the microstructures of samples deformed to progressively higher strains at -10, -20 and -30 C. *The Cryosphere*, **14**(11), 3875–3905, ISSN 1994-0424 (doi: 10.5194/tc-14-3875-2020)

Gardner AS, Moholdt G, Scambos T, Fahnstock M, Ligtenberg S, van den Broeke M and Nilsson J (2018) Increased West Antarctic and unchanged East Antarctic ice discharge over the last 7 years. *The Cryosphere*, **12**(2), 521–547, ISSN 1994-0424 (doi: 10.5194/tc-12-521-2018)

Gerbi C, Mills S, Clavette R, Campbell S, Bernsen S, Clemens-Sewall D, Lee I, Hawley R, Kreutz K and Hruby K (2021) Microstructures in a shear margin: Jarvis Glacier, Alaska. *Journal of Glaciology*, 1–14, ISSN 0022-1430 (doi: 10.1017/jog.2021.62)

Glen J (1955) The creep of polycrystalline ice. *Proceedings of the Royal Society of London. Series A. Mathematical and Physical Sciences*, **228**(1175), 519–538, ISSN 0080-4630 (doi: 10.1098/rspa.1955.0066)

Goldsby D and Kohlstedt D (1997a) Grain boundary sliding in fine-grained Ice I. *Scripta Materialia*, **37**(9), 1399–1406, ISSN 13596462 (doi: 10.1016/S1359-6462(97)00246-7)

Goldsby DL and Kohlstedt DL (1997b) Flow of ice by Dislocation, Grain Boundary Sliding, and Diffusion Processes. *Lunar and Planetary Science*

Goldsby DL and Kohlstedt DL (2001) Superplastic deformation of ice: Experimental observations. *Journal of Geophysical Research: Solid Earth*, **106**(B6), 11017–11030, ISSN 01480227 (doi: 10.1029/2000JB900336)

Gow AJ, Meese DA, Alley RB, Fitzpatrick JJ, Anandakrishnan S, Woods GA and Elder BC (1997) Physical and structural properties of the Greenland Ice Sheet Project 2 ice core: A review. *Journal of Geophysical Research: Oceans*, **102**(C12), 26559–26575, ISSN 01480227 (doi: 10.1029/97JC00165)

Gudmundsson GH, Paolo FS, Adusumilli S and Fricker HA (2019) Instantaneous Antarctic ice sheet mass loss driven by thinning ice shelves. *Geophysical Research Letters*, **46**(23), 13903–13909, ISSN 0094-8276 (doi: 10.1029/2019GL085027)

Howat IM, Porter C, Smith BE, Noh MJ and Morin P (2019) The Reference Elevation Model of Antarctica. *The Cryosphere*, **13**(2), 665–674, ISSN 1994-0424 (doi: 10.5194/tc-13-665-2019)

Hudleston PJ (2015) Structures and fabrics in glacial ice: A review. *Journal of Structural Geology*, **81**, 1–27, ISSN 01918141 (doi: 10.1016/j.jsg.2015.09.003)

Jacka TH and Li Jun (1994) The steady-state crystal size of deforming ice. *Annals of Glaciology*, **20**(1958), 13–18, ISSN 02603055

Jellinek HH and Brill R (1956) Viscoelastic properties of ice. *Journal of Applied Physics*, **27**(10), 1198–1209, ISSN 00218979 (doi: 10.1063/1.1722231)

Jezek K, Alley R and Thomas (1985) Rheology of Glacier Ice. *Science*, **227**(4692), 1335–1337, ISSN 0036-8075 (doi: 10.1126/science.227.4692.1335)

Jones SJ and Brunet JG (1978) Deformation of Ice Single Crystals Close to the Melting Point. *Journal of Glaciology*, **21**(85), 445–455, ISSN 0022-1430 (doi: 10.3189/s0022143000033608)

King MD, Howat IM, Candela SG, Noh MJ, Jeong S, Noël BPY, van den Broeke MR, Wouters B and Negrete A (2020) Dynamic ice loss from the Greenland Ice Sheet driven by sustained glacier retreat. *Communications Earth Environment*, **1**(1), 1, ISSN 2662-4435 (doi: 10.1038/s43247-020-0001-2)

Kuiper EJN, De Bresser JH, Drury MR, Eichler J, Pennock GM and Weikusat I (2020a) Using a composite flow law to model deformation in the NEEM deep ice core, Greenland-Part 2: The role of grain size and premelting on ice deformation at high homologous temperature. *Cryosphere*, **14**(7), 2449–2467, ISSN 19940424 (doi: 10.5194/tc-14-2449-2020)

Kuiper EJN, Weikusat I, de Bresser JHP, Jansen D, Pennock GM and Drury MR (2020b) Using a composite flow law to model deformation in the NEEM deep ice core, Greenland – Part 1: The role of grain size and grain size distribution on deformation of the upper 2207 m. *The Cryosphere*, **14**(7), 2429–2448, ISSN 1994-0424 (doi: 10.5194/tc-14-2429-2020)

Lliboutry L (1969) The Dynamics of Temperature Glaciers from the Detailed Viewpoint. *Journal of Glaciology*, **56**(53)

Mellor M and Smith JH (1967) Creep of Snow and Ice. In *International Conference on Low Temperature Science*, 843–855

Mellor M and Testa R (1969a) Creep of Ice under Low Stress. *Journal of Glaciology*, **8**(52), 147–152, ISSN 0022-1430 (doi: 10.3189/S0022143000020815)

Mellor M and Testa R (1969b) Effect of Temperature on the Creep of Ice. *Journal of Glaciology*, **8**(52), 131–145, ISSN 0022-1430 (doi: 10.3189/s0022143000020803)

Meyer CR and Minchew BM (2018) Temperate ice in the shear margins of the Antarctic Ice Sheet: Controlling processes and preliminary locations. *Earth and Planetary Science Letters*, **498**, 17–26 (doi: 10.1016/j.epsl.2018.06.028)

Millstein JD, Minchew BM and Pegler SS (2022) Ice viscosity is more sensitive to stress than commonly assumed. *Communications Earth Environment*, **3**(1), 1–7 (doi: 10.1038/s43247-022-00385-x)

Minchew BM, Meyer CR, Robel AA, Gudmundsson GH and Simons M (2018) Processes controlling the downstream evolution of ice rheology in glacier shear margins: case study on Rutford Ice Stream, West Antarctica. *Journal of Glaciology*, **64**(246), 583–594 (doi: 10.1017/jog.2018.47)

Montagnat M and Duval P (2000) Rate controlling processes in the creep of polar ice, influence of grain boundary migration associated with recrystallization. *Earth and Planetary Science Letters*, **183**(1-2), 179–186, ISSN 0012821X (doi: 10.1016/S0012-821X(00)00262-4)

Montagnat M and Duval P (2004) Dislocations in ice and deformation mechanisms: From single crystals to polar ice. *Defect and Diffusion Forum*, **229**(January 2017), 43–54, ISSN 16629507 (doi: 10.4028/www.scientific.net/ddf.229.43)

Morlighem M, Rignot E, Binder T, Blankenship DD, Drews R, Eagles G, Eisen O, Ferraccioli F, Forsberg R, Fretwell P, Goel V, Greenbaum J, Gudmundsson H, Guo J, Gelm V, Hofstede C, Howat I, Humbert A, Jokat W, Karlsson N, Lee W, Matsuoka K, Millan R, Mouginot J, Paden J, Pattyn F, Roberts J, Rosier S, Ruppel A, Seroussi H, Smith E, Steinhage D, Sun B, van den Broeke M, van Ommen T, van Wessem M and Young D (2020) Deep glacial troughs and stabilizing ridges unveiled beneath the margins of the Antarctic ice sheet. *Nature Geoscience*, **13**, 132–137

Muguruma J (1969) Effects of surface condition on the mechanical properties of ice crystals. *Journal of Physics D: Applied Physics*, **2**(11), 1517–1525, ISSN 00223727 (doi: 10.1088/0022-3727/2/11/305)

Pettit EC and Waddington ED (2003) Ice flow at low deviatoric stress. *Journal of Glaciology*, **49**(166), 359–369, ISSN 0022-1430 (doi: 10.3189/172756503781830584)

Pimienta P and Duval P (1987) Rate Controlling Processes in the Creep of Polar Glacier Ice. *Le Journal de Physique Colloques*, **48**(C1), C1–243–C1–248, ISSN 0449-1947 (doi: 10.1051/jphyscol:1987134)

Qi C, Goldsby DL and Prior DJ (2017) The down-stress transition from cluster to cone fabrics in experimentally deformed ice. *Earth and Planetary Science Letters*, **471**, 136–147, ISSN 0012821X (doi: 10.1016/j.epsl.2017.05.008)

Ranganathan M, Minchew B, Meyer CR and Peč M (2021) Recrystallization of ice enhances the creep and vulnerability to fracture of ice shelves. *Earth and Planetary Science Letters*, **576**, 117219, ISSN 0012821X (doi: 10.1016/j.epsl.2021.117219)

Raraty L and Tabor D (1958) The adhesion and strength properties of ice. *Proceedings of the Royal Society of London. Series A. Mathematical and Physical Sciences*, **245**(1241), 184–201, ISSN 0080-4630 (doi: 10.1098/rspa.1958.0076)

Rignot E, Vaughan DG, Schmeltz M, Dupont T and Macayeal D (2002) Acceleration of Pine Island and Thwaites Glaciers, West Antarctica. *Annals of Glaciology*, **34**, 189–194, ISSN 0260-3055 (doi: 10.3189/172756402781817950)

Saruya T, Nakajima K, Takata M, Homma T, Azuma N and Goto-Azuma K (2019) Effects of microparticles on deformation and microstructural evolution of fine-grained ice. *Journal of Glaciology*, **65**(252), 531–541, ISSN 00221430 (doi: 10.1017/jog.2019.29)

Scambos TA (2004) Glacier acceleration and thinning after ice shelf collapse in the Larsen B embayment, Antarctica. *Geophysical Research Letters*, **31**(18), L18402, ISSN 0094-8276 (doi: 10.1029/2004GL020670)

Smith GD and Morland LW (1981) Viscous relations for the steady creep of polycrystalline ice. *Cold Regions Science and Technology*, **5**(2), 141–150, ISSN 0165232X (doi: 10.1016/0165-232X(81)90048-3)

Thorsteinsson T, Kipfstuhl J and Miller H (1997) Textures and fabrics in the GRIP ice core. *Journal of Geophysical Research: Oceans*, **102**(C12), 26583–26599, ISSN 21699291 (doi: 10.1029/97JC00161)

Tison JL and Hubbard B (2000) Ice crystallographic evolution at a temperate glacier: Glacier de Tsanfleuron, Switzerland. *Geological Society Special Publication*, **176**, 23–38, ISSN 03058719 (doi: 10.1144/GSL.SP.2000.176.01.03)

Treverrow A, Budd WF, Jacka TH and Warner RC (2012) The tertiary creep of polycrystalline ice: Experimental evidence for stress-dependent levels of strain-rate enhancement. *Journal of Glaciology*, **58**(208), 301–314, ISSN 00221430 (doi: 10.3189/2012JoG11J149)

Urai J, Means W and Lister G (1995) Dynamic Recrystallization of Minerals. *Geophysical Monograph Series*, **36**, 332–347

Van Wessem JM, Reijmer CH, Morlighem M, Mouginot J, Rignot E, Medley B, Joughin I, Wouters B, Depoorter MA, Bamber JL, Lenaerts JT, Van De Berg WJ, Van Den Broeke MR and Van Meijgaard E (2014) Improved representation of East Antarctic surface mass balance in a regional atmospheric climate model. *Journal of Glaciology*, **60**(222), 761–770, ISSN 00221430 (doi: 10.3189/2014JoG14J051)

Weertman J (1955) Theory of steady-state creep based on dislocation climb. *Journal of Applied Physics*, **26**(10), 1213–1217, ISSN 00218979 (doi: 10.1063/1.1721875)

Wilson C, Zhang Y and Stüwe K (1996) The effects of localized deformation on melting processes in ice. *Cold Regions Science and Technology*, **24**(2), 177–189, ISSN 0165232X (doi: 10.1016/0165-232X(95)00024-6)

Wilson CJ and Zhang Y (1996) Development of microstructure in the high-temperature deformation of ice. *Annals of Glaciology*, **23**, 293–302, ISSN 02603055 (doi: 10.3189/s0260305500013562)

Wingham DJ, Wallis DW and Shepherd A (2009) Spatial and temporal evolution of Pine Island Glacier thinning, 1995-2006. *Geophysical Research Letters*, **36**(17), 5–9, ISSN 00948276 (doi: 10.1029/2009GL039126)

Zeitz M, Levermann A and Winkelmann R (2020) Sensitivity of ice loss to uncertainty in flow law parameters in an idealized one-dimensional geometry. *Cryosphere*, **14**(10), 3537–3550, ISSN 19940424 (doi: 10.5194/tc-14-3537-2020)

Zeitz M, Winkelmann R and Levermann A (2021) Implications of flow law uncertainty for flow-driven ice-loss in Greenland under idealized warming pathways. *Preprint*, 1–21